JOURNAL OF COMPUTATIONAL PHYSICS 55, 1–32 (1984)

A Second-Order Godunov-Type Scheme for Compressible Fluid Dynamics

MATANIA BEN-ARTZI

Department of Mathematics, Technion–Israel Institute of Technology, Haifa 32000, Israel

AND

JOSEPH FALCOVITZ

Computation Division, Rafael Ballistic Center, P. O. Box 2250, Haifa 31021, Israel

Received December 9, 1982; revised August 25, 1983

A second-order accurate scheme for the integration in time of the conservation laws of compressible fluid dynamics is presented. Two related versions are proposed, one Lagrangian and the second direct Eulerian. They both share the common ingredient which is a full analytic solution for the time derivatives of flow quantities at a jump discontinuity, assuming initial nonvanishing slopes on both sides. While this solution is an extension of the solution to the classical Riemann problem, the resulting schemes are second-order extensions of Godunov's methods. In both cases, they are very simple to implement in computer codes. Several numerical examples are shown, where the only additional mechanism is a simple monotonicity algorithm.

1. INTRODUCTION

Consider the equations of an unsteady inviscid compressible flow in one space dimension written in conservation form,

$$U_t + \Phi(U)_x = 0,$$
$$U = \begin{pmatrix} \rho \\ \rho u \\ \rho(e + \frac{1}{2}u^2) \end{pmatrix}, \qquad \Phi(U) = \begin{pmatrix} \rho u \\ \rho u^2 + p \\ \rho u(e + \frac{1}{2}u^2) + pu \end{pmatrix}, \tag{1.1}$$

where u, ρ, e are velocity, specific density, and specific internal energy, respectively, and $p = p(e, \rho)$ is the pressure.

0021-9991/84 $3.00

Transforming to the Lagrangian coordinate $d\xi = \rho\, dx$, Eq. (1.1) takes the form,

$$V_t + \Psi(V)_\xi = 0, \qquad V = \begin{pmatrix} \frac{1}{\rho} \\ u \\ e + \frac{1}{2}u^2 \end{pmatrix}, \quad \Psi(V) = \begin{pmatrix} -u \\ p \\ pu \end{pmatrix}. \tag{1.2}$$

It is the purpose of this paper to present schemes of second-order accuracy for the initial value problems associated with either (1.1) or (1.2). In both cases our schemes are direct extensions of Godunov's well-known first-order method [7].

To illustrate our method let us consider first a single conservation law (f convex),

$$w_t + f(w)_x = 0. \tag{1.3}$$

As is customary in finite difference techniques, we use equally spaced grid points $x_i = i\,\Delta x$ and advance the solution by a fixed time increment Δt. Setting $x_{i+1/2} = \frac{1}{2}(x_i + x_{i+1})$ we define "cell i" as the interval $(x_{i-1/2}, x_{i+1/2})$ and let w_i^n be the average value of w over cell i at time $t_n = n\,\Delta t$. Suppose first that w is taken as piecewise constant at t_n, namely, constant in each cell i, with "jump discontinuities" at $x_{i+1/2}$. As is well known, such an initial discontinuity gives rise to a solution of (1.3) which is either a shock or a centered rarefaction wave. As long as interaction with neighboring waves does not occur (thus limiting Δt) constant values of w are propagated along straight lines emanating from the point of discontinuity. Denoting by $w_{i+1/2}^{n+1/2} = w_{i+1/2}^n$ the value along $x = x_{i+1/2}$ (in case of a stationary shock take the appropriate one-sided value), one obtains a difference scheme for (1.3),

$$w_i^{n+1} - w_i^n = -\frac{\Delta t}{\Delta x}\,(f(w)_{i+1/2}^{n+1/2} - f(w)_{i-1/2}^{n+1/2}). \tag{1.4}$$

Suppose next that w is discretized not as a piecewise constant function but rather a piecewise linear function, so that in each cell i a constant value $(\partial w/\partial x)_i^n$ is assumed along with w_i^n. The difference equation (1.4) may still be used, provided the jump discontinuity is resolved and a suitable value $f(w)_{i+1/2}^{n+1/2}$ is obtained. If second-order accuracy is desired, this value must be determined within $O(\Delta t^2)$ or otherwise stated, we must have

$$f(w)_{i+1/2}^{n+1/2} = f(w)_{i+1/2}^n + \frac{\Delta t}{2}\left(\frac{\partial}{\partial t} f(w)\right)_{i+1/2}^n. \tag{1.5}$$

Here $f(w)_{i+1/2}^n$ is the instantaneous value of $f(w)$ immediately after resolving the discontinuity, obtained as the solution of the previous case (constant values on both sides) at $x = x_{i+1/2}$. The corresponding constant values are naturally $w_i^n + (\Delta x/2)(\partial w/\partial x)_i^n$ and $w_{i+1}^n - (\Delta x/2)(\partial w/\partial x)_{i+1}^n$. It remains to consider the time derivative in (1.5), which reflects the nonuniformity of data on both sides. In the

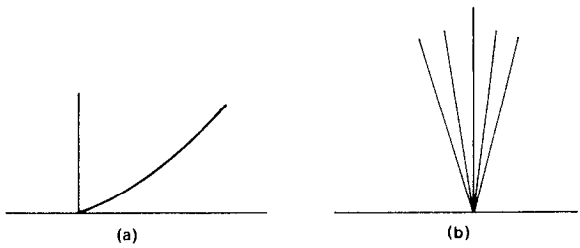

FIG. 1. Resolution of a discontinuity for a single conservation law. (a) nonsonic case, (b) sonic case.

present case it is easy to compute. Indeed, Fig. 1 displays the only two possibilities. In Fig. 1a a wave (either a shock or a rarefaction) propagates to the right, leaving the line $x = x_{i+1/2}$ in a region where w is smooth, so that from (1.3) we get,

$$\left(\frac{\partial f(w)}{\partial t}\right)^n_{i+1/2} = -\left| f'\left(w_i^n + \frac{\Delta x}{2}\left(\frac{\partial w}{\partial x}\right)^n_i\right)\right|^2 \left(\frac{\partial w}{\partial x}\right)^n_i. \tag{1.6}$$

In Fig. 1b the line $x = x_{i+1/2}$ is contained in a centered rarefaction wave. Later on we refer to this case as the *sonic case* and realize that in the fluid dynamical context it is the most difficult case. However, in the present case we are fortunate since, regardless of the distribution of w on both sides the characteristics are straight lines carrying constant values of w, hence, $(\partial f(w)/\partial t)^n_{i+1/2} = 0$ (which means in numerical terms that at sonic points the scheme is first order).

We have discussed Eq. (1.3) at some length since in principle our schemes for (1.1), (1.2) are precisely analogous to (1.4), where the fluxes halfway in time are evaluated by an equivalent of (1.5). This naturally leads to consideration of the terms in the right-hand side of (1.5) in the case of a system.

The classical *Riemann problem* (RP) is [5, Sect. 80]:

Given two constant states $U_\pm$, *find a solution of the initial value problem* (1.1) *so that* $U(x, 0) = U_\pm$ *for* $\pm x > 0$.

Let us recall briefly the main features of the solution. Generally speaking, the jump discontinuity breaks up into a contact discontinuity which separates two waves, each of which may be either a shock or a rarefaction. The flow field between the waves is constant and the entire solution is self-similar in the sense that all quantities are functions of x/t only. We shall find it convenient in what follows to denote this solution by $R(x/t; U_+, U_-)$.

As was the case with the single conservation law, we realize that in order to achieve second-order accuracy one has to deal with the *generalized Riemann problem* (GRP) formulated as follows:

Given two linearly distributed states $U_\pm(x)$, *find a solution of the initial value problem* (1.1) *such that* $U(x, 0) = U_\pm(x)$, *for* $\pm x > 0$.

Of course in this case we do not expect a simple "global" solution, but rather a "good local approximation" in terms to be specified later. Our basic hypothesis is the following:

Define the "associated RP" as the Riemann problem with constant initial states given by $U_{\pm} = \lim_{x \to 0\pm} U_{\pm}(x)$. Then locally, the wave pattern for the GRP is the same as that of the "associated RP," meaning that if a solution of one problem involves a shock propagating to the left then so does the other, etc. Furthermore, the two solutions converge to the same values at the point of singularity. Symbolically, if $U(x, t)$ is the solution to the GRP,

$$\lim_{t \to 0} U(x, t) = R(p; U_+, U_-) \qquad \text{along } \frac{x}{t} = p = \text{const.} \tag{1.7}$$

Observe, however, that some features of the solution of the RP are lost in the case of the GRP, even locally. Thus, the solution is no longer self-similar, characteristics are not straight lines, and centered rarefaction waves are not necessarily isentropic.

Let us now turn back to the problem of associating second-order accurate difference schemes with (1.1), (1.2). Following the same line of thought leading to (1.5) we conclude that what is needed is the time derivative $\partial \Phi(U)/\partial t$ (or, for (1.2), $\partial \Psi(V)/\partial t$) at the singularity, for a solution of the GRP.

The main building block in our scheme is an analytic derivation of the above time derivatives, both in the Eulerian and Lagrangian frameworks. In the process of achieving this goal we give a full acount of the behavior (to within $O(\Delta t^2)$) of the solution to the GRP and, in particular, a detailed resolution of the nonisentropic rarefaction fans. It turns out that the entire solution can be expressed in closed form for a γ-law equation-of-state and involves only simple integrations in the most general case.

Once the solution to the GRP is established, the analogues of (1.4), (1.5) are set up. The resulting schemes are simple and straightforward. In particular, let us stress the following points:

(a) A standard Riemann problem is solved *once* per cell boundary per time step. All subsequent "programming decisions" are made solely on the basis of this solution.

(b) A "plug-in" procedure, using the explicit analytic solution, is used in order to compute time derivatives of flow quantities. Cell averages are then advanced conservatively and slopes are updated by differencing new values at cell boundaries.

(c) No accessory technique is used except for a simple monotonicity algorithm. In particular, no other dissipative mechanism is incorporated.

The paper is organized as follows. In Section 2 we outline the basic steps needed in the implementation of the present scheme. Section 3 summarizes the notation and conventions used throughout the paper. The analytic resolution of a centered rarefaction wave is discussed in Section 4. Our method is based on a "propagation of singularities" argument [6, Sect. V.1], that is, the observation that along a characteristic curve the jump in the highest order transversal derivative satisfies an ordinary differential equation. In our case, the characteristic curve shrinks to a point at the singularity. In Section 5 we carry out the computation of the time derivatives of the

pressure and velocity along the contact discontinuity (note that they are continuous across the discontinuity). Looking at Eq. (1.2) we see that these derivatives are all we need for the time derivative of the flux vector in the Lagrangian frame. Thus, Section 6 concludes the discussion of our Lagrangian scheme. It turns out that this scheme is closely related to the one proposed by van Leer in [11], which seems to have initiated the interest in second-order Godunov methods. In Appendix A we prove that van Leer's equations are second-order approximations to the analytic solution, and in Appendix C we give some more details needed in the implementation of the Lagrangian scheme. The Eulerian scheme is discussed in Section 7. Essentially, it shares many common features with the Lagrangian case, except for the appearance of the *sonic case*, that is, when the grid line $x = x_{i+1/2}$ is contained in a rarefaction fan. The characteristics emanating from the singularity are not straight lines and the grid line intersects every one of them nontangentially when expressed in characteristic coordinates. The evaluation of the time derivative in this case plays an important role in the above-mentioned analytic solution. While the results are given in Section 7, some proofs are relegated to Appendix B, and some additional details are given in Appendix D. Incidentally, in dealing with the Eulerian sonic case we use the fact that in the solution of the "associated RP" the flux is stationary (see (7.16)). This simplifies the computation considerably. Recently, a number of direct Eulerian second-order "upstream" methods were proposed by Colella [2], Colella–Woodward [3], and Harten [8, 9]. They all differ from ours in that they do not handle directly time derivatives at the singularity. The concluding Section 8 is devoted to some numerical examples. We discuss (a) Sod's example [10] in both Lagrangian and Eulerian frameworks, (b) an almost stationary very strong shock in Eulerian coordinates [3], (c) two interacting blast waves [4].

2. Outline of the Numerical Scheme

Figure 2 displays a typical distribution of a flow variable at any given time t_n. As in the previous section, cell midpoints are labeled by integral values i, whereas the half-integer index $i + \frac{1}{2}$ is used for cell boundaries. We denote by Q any one of the

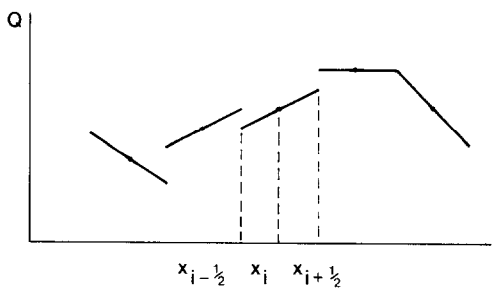

FIG. 2. Typical distribution of flow variables in cells.

flow variables and use subscripts to indicate spatial location and superscripts for time. Thus Q_i^n, $Q_{i+1/2}^{n+1/2}$ stand for the values of Q at $(i\Delta x, n\Delta t)$, $((i+\frac{1}{2})\Delta x, (n+\frac{1}{2})\Delta t)$, the first being the average in cell i, while the second is the cell boundary value averaged in time. Obviously, when dealing with Eq. (1.2) Δx is replaced by $\Delta\xi$, $\partial Q/\partial x$ by $\partial Q/\partial\xi$, etc. We denote by $(\Delta Q)_i^n$ the variation of Q in cell i. The (constant) slope of Q in that cell is obtained as $(\partial Q/\partial x)_i^n = (1/\Delta x)(\Delta Q)_i^n$. As was explained in Section 1, the main ingredient of the scheme is the computation (via the solution of the GRP) of $(\partial Q/\partial t)_{i+1/2}^n$, the instantaneous rate of change of Q, following the resolution of the jump discontinuity.

Our strategy for solving (1.1), (1.2) numerically may now be summarized as follows (we formulate in terms of (1.1)).

Step A. Define boundary values at $i+\frac{1}{2}$ by

$$U_{\pm} = U_{i+1/2\pm1/2}^n \mp \tfrac{1}{2}(\Delta U)_{i+1/2\pm1/2}^n. \tag{2.1}$$

Use the solution of the RP (see Sect. 1) in order to define

$$U_{i+1/2}^n = R(0; U_+, U_-). \tag{2.2}$$

Observe that the line $x = x_{i+1/2}$ may represent a discontinuity for the RP (in particular $\xi = \xi_{i+1/2}$ is always a contact discontinuity) in which case $U_{i+1/2}^n$ is double-valued. In all cases the flux is continuous.

Step B. Using the given slopes $(\Delta U)_i^n$, $(\Delta U)_{i+1}^n$, in the analytic solution of the GRP, compute $(\partial U/\partial t)_{i+1/2}^n$ and in particular $(\partial \Phi(U)/\partial t)_{i+1/2}^n$.

Step C. Set

$$\Phi(U)_{i+1/2}^{n+1/2} = \Phi(U_{i+1/2}^n) + \frac{\Delta t}{2}\left(\frac{\partial \Phi(U)}{\partial t}\right)_{i+1/2}^n, \tag{2.3}$$

$$U_i^{n+1} = U_i^n - \frac{\Delta t}{\Delta x}\left[\Phi(U)_{i+1/2}^{n+1/2} - \Phi(U)_{i-1/2}^{n+1/2}\right]. \tag{2.4}$$

Step D. To update slopes of $Q = \rho, p, u$, use the following procedure,

$$\begin{aligned} Q_{i+1/2}^{n+1} &= Q_{i+1/2}^n + \Delta t\left(\frac{\partial Q}{\partial t}\right)_{i+1/2}^n, \\ (\Delta Q)_i^{n+1} &= Q_{i+1/2}^{n+1} - Q_{i-1/2}^{n+1} \end{aligned} \tag{2.5}$$

(with obvious care when $Q_{i\pm1/2}^{n+1}$ is double-valued). These slopes are now modified by a monotonicity algorithm which secures that they vanish at extremal points of the (average) Q distribution and that in monotonic distributions, for every i, the cell-boundary values $Q_{i-1/2}^{n+1}$, $Q_{i+1/2}^{n+1}$ are in line with the values Q_{i-1}^{n+1}, Q_i^{n+1}, Q_{i+1}^{n+1} (see [11] for details).

There is an extensive discussion in the literature of algorithms for the numerical implementation of Step A, that is, finding an "optimal Riemann solver" (see [1, 10, 11]). We shall, therefore, omit the details here. The solution of the RP involves, in general, two waves separated by a contact dicontinuity. As was explained in the Introduction, our basic hypothesis in setting up the initial conditions for Step B is that the nature of the *wave pattern* is that obtained in $R(\cdot;\ U_+, U_-)$. This hypothesis is applicable only in the immediate neighborhood of the singularity and has no further quantitative implications on the GRP solution except for (1.7). In particular, characteristics and shock trajectories are curvilinear and carry nonuniform values of the flow variables.

Once Step B is taken care of, the remaining two steps are straightforward and we shall not discuss them in detail. Thus, the rest of the paper is devoted to carrying out the analysis required in Step B, both in the Lagrangian and Eulerian frameworks. Since the indices (i, n) are now fixed, we suppress them in the sequel. For notational convenience we take $x = \xi = t = 0$ at the point of singularity and refer to the values U_+, U_- (see (2.1)) as the "right" and "left" values, respectively, and denoted U_r, U_l. A similar convention is employed for the slopes on both sides. For the reader's convenience the simplified notation to be used henceforth is listed in Section 3.

3. Basic Notations

In addition to the basic flow variables introduced in Section 1 we shall also make use of the speed of sound c and the "Lagrangian" speed of sound $g = \rho c$. Our analysis will be carried out in terms of a general equation-of-state. However, the results are particularly simple when applied to the γ-law equation, namely,

$$p = (\gamma - 1)\rho e, \qquad \gamma > 1. \tag{3.1}$$

We shall always write down the explicit form of the formulae for this special case. Following van Leer's convention, we shall add the label γ to the numbers of those equations which are specialized to the γ-law case.

The Lagrangian coordinate ξ is defined by $d\xi = \rho\, dx$ and we assume that the discontinuity is located at $x = \xi = 0$, $t = 0$. The subsequent flow (for the GRP) is displayed in Fig. 3, which uses the (ξ, t) plane. It is assumed that a centered rarefaction wave (CRW) propagates to the left and a shock travels to the right. The line $\xi = 0$ is a contract discontinuity. As before, we denote by $Q(\xi, t)$ any one of the flow variables.

The notations to be used in the sequel are listed in Table I. We use the setup of Eq. (1.2). The analogous notations for (1.1) should be clear. (See also Fig. 3.).

Remark. Note carefully the distinction between the various groups of quantities.

Q_r, Q_l, $(\partial Q/\partial \xi)_r$, $(\partial Q/\partial \xi)_l$ are the given initial data (V_r, V_l correspond to $V_\pm$ analogously to (2.1)).

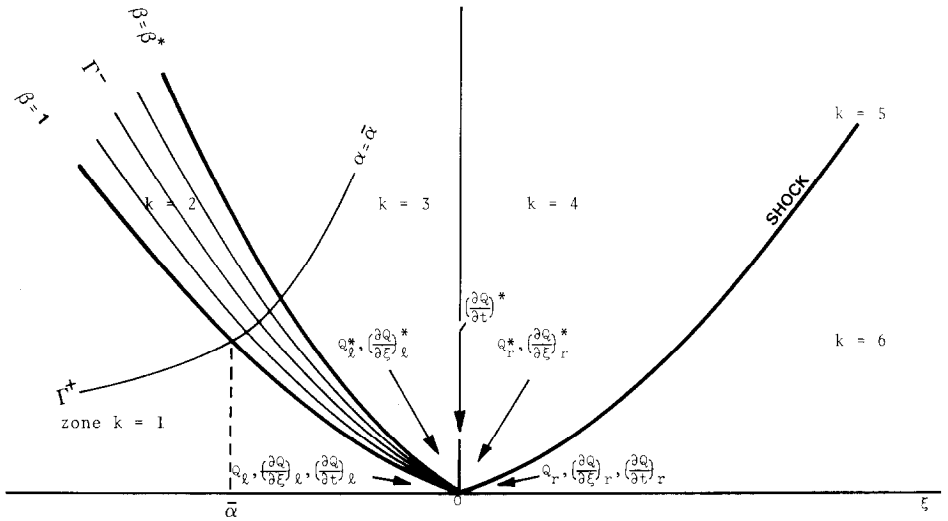

FIG. 3. Wave pattern and related quantities (used in Table I, Sect. 3) for the resolution of a discontinuity in Lagrangian coordinates. Note the partition into zones $k = 1$ to 6, where the waves constitute zones $k = 2$ and 5.

TABLE I

Notations

Symbol	Definition
Q_r, Q_l	$\lim Q(\xi, 0)$ as $\xi \to 0\pm$
$\left(\frac{\partial Q}{\partial \xi}\right)_r, \left(\frac{\partial Q}{\partial \xi}\right)_l$	Constant slopes for $\pm\xi > 0$
$R(\cdot; V_+, V_-)$	Solution of the RP
V^*	$R(0; V_r, V_l)$
Q_r^*, Q_l^*	Right and left values in case Q discontinuous across $(\xi = 0)$, $Q = \rho, c, g = \rho c$
$\left(\frac{\partial Q}{\partial t}\right)^*$	$\frac{\partial}{\partial t} Q(\xi, t)$ along $\xi = 0$ at $t = 0+$
$\left(\frac{\partial Q}{\partial t}\right)_r^*, \left(\frac{\partial Q}{\partial t}\right)_l^*$	Right and left values of $\left(\frac{\partial Q}{\partial t}\right)^*$ for discontinuous Q
$\left(\frac{\partial Q}{\partial \xi}\right)_r^*, \left(\frac{\partial Q}{\partial \xi}\right)_l^*$	$\lim_{t\to 0+} \lim_{\xi\to 0+} \frac{\partial Q(\xi, t)}{\partial \xi}, \lim_{t\to 0+} \lim_{\xi\to 0-} \frac{\partial Q(\xi, t)}{\partial \xi}$
$\left(\frac{\partial Q}{\partial t}\right)_l$	$\lim_{\xi\to 0-} \frac{\partial Q(\xi, t)}{\partial t}\Big\|_{t-0}$
$\left(\frac{\partial Q}{\partial t}\right)_r$	$\lim_{\xi\to 0+} \frac{\partial Q(\xi, t)}{\partial t}\Big\|_{t=0}$
U_0	$R(0; U_r, U_l)$ (only in Sect 7)
$\left(\frac{\partial Q}{\partial t}\right)_0$	$\frac{\partial}{\partial t} Q(x, t)$ along $x = 0$ at $t = 0+$ (only in Sect. 7)

Q^*, Q_r^*, Q_l^* result from the solution of the Riemann problem, $R(\cdot; V_r, V_l)$, in Lagrangian coordinates.

$(\partial Q/\partial t)^*$, $(\partial Q/\partial \xi)_r^*$, $(\partial Q/\partial \xi)_l^*$ result from the solution of the generalized Riemann problem (GRP).

$(\partial Q/\partial t)_l, (\partial Q/\partial t)_r$ represent limits of time derivatives taken ahead of the waves and can therefore be expressed by initial spatial derivatives in view of (1.2).

$Q_0, (\partial Q/\partial t)_0$ apply to the Eulerian case only (Sect. 7). They may be double-valued if $x = 0$ is a line of discontinuity for the RP.

4. Resolution of a Centered Rarefaction Wave (CRW)

In this section we deal with the most important feature of the solution of the GRP, namely, the resolution of the nonisentropic CRW. We assume that (see Fig. 3) the CRW propagates to the left and work in the (ξ, t) plane. As shown in Fig. 3, we introduce some characteristic notation. Let $\Gamma^{\pm}$ be the characteristic families of (1.2) corresponding to the eigenvalues $\pm g = \pm \rho c$. In the RP the Γ^-, Γ^+ curves are, respectively, straight lines and hyperbolas [5, Sect. 47]. The slopes of the Γ^- lines extend from $-g_l$ at the head to $-g_l^*$ at the tail of the rarefaction. We can therefore parametrize the CRW by characteristic coordinates (α, β) such that

$$\alpha = -(-g_l \xi t)^{1/2}, \qquad \beta = -g_l^{-1} \frac{\xi}{t}. \tag{4.1}$$

Geometrically, β is the slope of the Γ^--line normalized so that $\beta = 1$ at the head and extending down to $\beta^* = g_l^*/g_l \leqslant 1$. The coordinate α is the ξ coordinate of the intersection of the Γ^+-curve with the head characteristic $\beta = 1$. Inverting the relations (4.1) yields

$$\xi = \alpha \beta^{1/2}, \qquad t = -g_l^{-1} \alpha \beta^{-1/2}. \tag{4.2}$$

Passing to the GRP both $\Gamma^{\pm}$-families are distorted. We retain our definition of (α, β) as parameters along (Γ^-, Γ^+) curves, respectively, interpreting β as the normalized slope as $t \to 0$, α as the ξ-coordinate of the intersection with $\beta = 1$. The amount of slope distortion of the characteristics is obviously $O(\alpha)$, hence, the point of intersection of any particular Γ^+ curve with the curve $\beta = 1$ is removed by $O(\alpha^2)$ from the corresponding point in the RP. It is then geometrically evident (and is easily established analytically in view of (1.7) and the characteristic relations) that $\partial \xi/\partial \alpha$, $\partial t/\partial \alpha$ along Γ^- curves tend to the same values (as $\alpha \to 0$) as implied by (4.2). Hence, in the GRP,

$$\xi = \alpha \beta^{1/2} + \varepsilon(\alpha, \beta)\alpha^2, \qquad t = -g_l^{-1} \alpha \beta^{-1/2} + \eta(\alpha, \beta)\alpha^2, \tag{4.3}$$

where $\varepsilon(\alpha, \beta)$, $\eta(\alpha, \beta)$ are smooth functions in $[-\alpha_0, 0] \times [\beta^*, 1]$ for some $\alpha_0 > 0$.

(The values of $\varepsilon(0,\beta)$, $\eta(0,\beta)$ play an important role in the sonic case, see Appendix B.) Note that the slopes of Γ^- curves at the singularity coincide with those of the associated RP by (1.7). For any flow variable Q we let $Q(\alpha,\beta)$ be its representation in characteristic coordinates throughout the CRW. In terms of these coordinates Q is well behaved and smooth up to the singularity $\alpha = 0$. Starting with the velocity u, we have

THEOREM 4.1. *Let* $a(\beta) = (\partial u/\partial\alpha)(0,\beta)$, $\beta^* \leqslant \beta \leqslant 1$. *Then* $a(\beta)$ *satisfies a relation of the form*

$$a'(\beta) + H(\beta) = 0, \qquad \beta \in [\beta^*, 1], \tag{4.4}$$

where $H(\beta)$ *is a function that can be explicitly determined from the equation of state and the initial conditions ahead of the rarefaction. If the entropy ahead of the rarefaction is uniform* $H(\beta) \equiv 0$.

Equation (4.4) is supplemented by the condition

$$a(1) = \left(\frac{\partial u}{\partial \xi}\right)_l + g_l^{-1}\left(\frac{\partial p}{\partial \xi}\right)_l. \tag{4.5}$$

For a γ-law equation of state we get

$$H(\beta) = \left| \frac{\gamma+1}{2c_l}\left(\frac{\partial p}{\partial \xi}\right)_l - \left(\frac{\partial g}{\partial \xi}\right)_l \right| \cdot \frac{1}{\rho_l(\gamma+1)}\beta^{(1/2)-(2/(\gamma+1))}, \tag{4.6}$$

so that in this case,

$$a(\beta) = a(1) + \frac{2}{g_l(3\gamma-1)}\left[c_l\left(\frac{\partial g}{\partial \xi}\right)_l - \frac{\gamma+1}{2}\left(\frac{\partial p}{\partial \xi}\right)_l\right] \cdot (\beta^{3\gamma-1)/2(\gamma+1)} - 1). \tag{4.7}$$

Proof. The characteristic relations along $\Gamma^{\pm}$ are expressed by

$$\frac{\partial u}{\partial \beta} + \frac{1}{g}\frac{\partial p}{\partial \beta} = 0, \qquad \frac{\partial u}{\partial \alpha} - \frac{1}{g}\frac{\partial p}{\partial \alpha} = 0. \tag{4.8}$$

Differentiate the first equation with respect to α, the second with respect to β, eliminate p, and set $\alpha = 0$ to obtain

$$2g(0,\beta)\,a'(\beta) + \frac{\partial g(0,\beta)}{\partial \beta}a(\beta) + \frac{\partial g(0,\beta)}{\partial \alpha}\frac{\partial u(0,\beta)}{\partial \beta} = 0. \tag{4.9}$$

Since the CRW is nonisentropic, it is impossible to compute g_α merely from p_α. So to eliminate g_α we proceed as follows: Given a state (g_0, p_0) let

$$g = G(g_0, p_0, p) \tag{4.10}$$

be the isentropic curve through (g_0, p_0). For a point (α, β), $\alpha < 0$, let $\xi(\alpha, \beta)$ be its ξ-coordinate as expressed by (4.3), and denote by

$$\begin{aligned} p_0(\alpha, \beta) &= p_l + \left(\frac{\partial p}{\partial \xi}\right)_l \cdot \xi(\alpha, \beta), \\ g_0(\alpha, \beta) &= g_l + \left(\frac{\partial g}{\partial \xi}\right)_l \cdot \xi(\alpha, \beta), \end{aligned} \tag{4.11}$$

the initial values of p, g at $\xi(\alpha, \beta)$. Since the flow is isentropic along the streamline $\xi = \text{const.}$, we conclude from (4.10), (4.11) that

$$g(\alpha, \beta) = G(g_0(\alpha, \beta), p_0(\alpha, \beta), p(\alpha, \beta)). \tag{4.12}$$

Differentiating this equation with respect to α and setting $\alpha = 0$ we have

$$\begin{aligned} g_\alpha(0, \beta) &= \left[G_{g_0}(g_l, p_l, p(0, \beta)) \left(\frac{\partial g}{\partial \xi}\right)_l + G_{p_0}(g_l, p_l, p(0, \beta)) \left(\frac{\partial p}{\partial \xi}\right)_l \right] \frac{\partial \xi(0, \beta)}{\partial \alpha} \\ &\quad + G_p(g_l, p_l, p(0, \beta)) \frac{\partial p(0, \beta)}{\partial \alpha} \\ &= A(\beta) \cdot \beta^{1/2} + g(0, \beta)\, G_p(g_l, p_l, p(0, \beta))\, a(\beta), \end{aligned} \tag{4.13}$$

where we have denoted by $A(\beta)$ the term in square brackets and made use of (4.3) in the first term and (4.8) in the second term. Inserting this expression in (4.9) and using (4.8) again, we see that the coefficient of $a(\beta)$ is given by

$$E(\beta) = \frac{\partial g(0, \beta)}{\partial \beta} - G_p(g_l, p_l, p(0, \beta)) \frac{\partial p(0, \beta)}{\partial \beta}.$$

But $E(\beta) \equiv 0$. Indeed, by (1.7) $p(0, \beta)$, $g(0, \beta)$, $\beta^* \leqslant \beta \leqslant 1$, are obtained in the solution of the RP for V_l, V_r and, therefore, represent isentropic states, namely, $g(0, \beta) = G(g_l, p_l, p(0, \beta))$. Differentiating this equality we get $E(\beta) = 0$. Thus, Eq. (4.4) is established with

$$H(\beta) = \tfrac{1}{2} g(0, \beta)^{-1} \beta^{1/2} A(\beta) \frac{\partial}{\partial \beta} u(0, \beta). \tag{4.14}$$

If the entropy ahead of the rarefaction is uniform then all states $p_0(\alpha, \beta)$, $g_0(\alpha, \beta)$ are isentropic, hence, $g(0, \beta) = G(g_0(\alpha, \beta), p_0(\alpha, \beta), p(0, \beta))$. Differentiating with respect to α and setting $\alpha = 0$, we get $A(\beta) = 0$, hence, $H(\beta) = 0$ in this case.

To establish (4.5) we use the chain rule and Eqs. (4.3), (1.2) to deduce,

$$a(1) = \frac{\partial u(0, 1)}{\partial \alpha} = \left(\frac{\partial u}{\partial \xi}\right)_l \frac{\partial \xi(0, 1)}{\partial \alpha} + \left(\frac{\partial u}{\partial t}\right)_l \frac{\partial t(0, 1)}{\partial \alpha} = \left(\frac{\partial u}{\partial \xi}\right)_l + g_l^{-1} \left(\frac{\partial p}{\partial \xi}\right)_l.$$

Now, in view of (1.7) the flow variables at $\alpha = 0$ are those obtained from the RP solution. The slope of a Γ^--curve is $-g$, so from (4.1) we get

$$g(0, \beta) = g_l \beta. \tag{4.15}$$

Specializing (4.10) to the γ-law relation we have

$$g = g_0 \left(\frac{p}{p_0}\right)^{(\gamma+1)/2\gamma},$$

and the well-known solution of a centered rarefaction wave in this case becomes

$$\begin{aligned} &p(0, \beta) = p_l \beta^{2\gamma/(\gamma+1)}, \qquad c(0, \beta) = c_l \beta^{(\gamma-1)/(\gamma+1)}, \\ &u(0, \beta) = u_l + \frac{2}{\gamma - 1} c_l - \frac{2}{\gamma - 1} c(0, \beta) = u_l + \frac{2c_l}{\gamma - 1}(1 - \beta^{(\gamma-1)/(\gamma+1)}). \end{aligned} \tag{4.16$_\gamma$}$$

Incorporating these expressions in (4.14) we get (4.6$_\gamma$), and (4.7$_\gamma$) is obtained by integrating (4.4). This concludes the proof of the theorem.

Once $a(\beta) = \partial u(0, \beta)/\partial \alpha$ is known, the other derivatives at the singularity are easily determined. Corresponding to (4.10), we let

$$\rho = J(\rho_0, p_0, p) \tag{4.17}$$

be the isentropic curve through a state (ρ_0, p_0). For a γ-law case it reads $\rho = \rho_0 (p/p_0)^{1/\gamma}$. We have

COROLLARY 4.2. *The following are the expressions for $\partial Q(\alpha, \beta)/\partial \alpha$ at the singularity $\alpha = 0$ for the various flow variables, both for a general equation of state and a γ-law case. Recall that $a(\beta) = \partial u(0, \beta)/\partial \alpha$ is given by* (4.4).

$$\frac{\partial p(0, \beta)}{\partial \alpha} = g_l \beta a(\beta), \tag{4.18}$$

$$\begin{aligned} \frac{\partial g(0, \beta)}{\partial \alpha} = &\left[G_{g_0}(g_l, p_l, p(0, \beta)) \left(\frac{\partial g}{\partial \xi}\right)_l + G_{p_0}(g_l, p_l, p(0, \beta)) \left(\frac{\partial p}{\partial \xi}\right)_l \right] \beta^{1/2} \\ &+ g_l \beta G_p(g_l, p_l, p(0, \beta))\, a(\beta), \end{aligned} \tag{4.19}$$

$$\frac{\partial g(0, \beta)}{\partial \alpha} = \left[\left(\frac{\partial g}{\partial \xi}\right)_l - \frac{\gamma + 1}{2c_l} \left(\frac{\partial p}{\partial \xi}\right)_l \right] \beta^{3/2} + \frac{\gamma + 1}{2} \rho_l a(\beta)\, \beta^{2/(\gamma+1)}, \tag{4.20$_\gamma$}$$

$$\begin{aligned} \frac{\partial \rho(0, \beta)}{\partial \alpha} = &\left[J_{\rho_0}(\rho_l, p_l, p(0, \beta)) \left(\frac{\partial \rho}{\partial \xi}\right)_l + J_{p_0}(\rho_l, p_l, p(0, \beta)) \left(\frac{\partial p}{\partial \xi}\right)_l \right] \beta^{1/2} \\ &+ g_l \beta c(0, \beta)^{-2} a(\beta), \end{aligned} \tag{4.21}$$

$$\frac{\partial \rho(0, \beta)}{\partial \alpha} = \rho_l \beta^{2/(\gamma+1)} \left[\left(\rho_l^{-1} \left(\frac{\partial \rho}{\partial \xi}\right)_l - (\gamma p_l)^{-1} \left(\frac{\partial p}{\partial \xi}\right)_l \right) \beta^{1/2} + c_l^{-1} \beta^{(1-\gamma)/(\gamma+1)} a(\beta) \right]. \tag{4.22$_\gamma$}$$

Proof. Equation (4.18) is the combination of (4.8) and (4.15). Equation (4.19) is just (4.13) if we note (4.15). To establish (4.21) we proceed as in (4.13) and get the analogue of (4.19) with G replaced by J. By the definition of the speed of sound $c^{-2} = J_p$, yielding (4.21) (note that (ρ_l, p_l) and $(\rho(0,\beta), p(0,\beta))$ have the same entropy). Finally, (4.20_γ), (4.22_γ) are derived from the specialized formulae for J, G.

Remark. Notice that given $\beta_0 \in [\beta^*, 1]$, the value of $a(\beta_0)$, hence, also for all $\partial Q(0,\beta_0)/\partial\alpha$, depends only on the flow ahead of the characteristic $\beta = \beta_0$, that is, data for $\xi < 0$ and $a(\beta)$ for $\beta_0 \leqslant \beta \leqslant 1$. This of course reflects the fact that no sonic signal reaches the characteristic from the other side.

5. Time Derivatives of p, u on the Interface

In this section we assume the situation is as displayed in Fig. 3 and compute $(\partial p/\partial t)^*$, $(\partial u/\partial t)^*$. Basically we follow the ideas of van Leer [11] and obtain these values as solutions of two linear equations. In Appendix A we study the connection between our approach and that of van Leer.

Let $W > 0$ be the (Lagrangian) shock speed and denote by Q_+ the preshock value of Q. Let the $(p-u)$ Hugoniot relation be written in the form

$$K(u, p, u_+, p_+, \rho_+) = 0.$$

Since it holds identically we may differentiate along the shock trajectory to get

$$\left(\frac{\partial}{\partial t} + W\frac{\partial}{\partial \xi}\right) K(u, p, u_+, p_+, \rho_+) = 0. \tag{5.1}$$

The solutions in the regions adjacent to the shock front are continuously differentiable up to the front. Hence, the time derivatives of u_+, p_+, ρ_+ may be replaced by ξ-derivatives using (1.2) and the adiabatic nature of the flow along $\xi = \text{const.}$,

$$\frac{\partial}{\partial t} u_+ = -\frac{\partial}{\partial \xi} p_+, \qquad \frac{\partial}{\partial t} \rho_+ = -\rho_+^2 \frac{\partial}{\partial \xi} u_+, \qquad \frac{\partial}{\partial t} p_+ = -g_+^2 \frac{\partial}{\partial \xi} u_+.$$

Similarly, in the post shock region $(\partial/\partial\xi)(u, p) = (-g^{-2}(\partial p/\partial t), -(\partial u/\partial t))$. Now we let $t \to 0$ and use that

$$\frac{\partial}{\partial t}(u, p) \to \left(\left(\frac{\partial u}{\partial t}\right)^*, \left(\frac{\partial p}{\partial t}\right)^*\right),$$

$$\frac{\partial}{\partial \xi} Q_+ \to \left(\frac{\partial Q}{\partial \xi}\right)_r.$$

Also, by (1.7), as $t \to 0$ the postshock solution $V(\xi, t)$ tends to $V^* = R(0; V_r, V_l)$ while W converges to $W_r = (p^* - p_r)/(u^* - u_r)$. Thus Eq. (5.1) reduces to a linear

relation for $(\partial u/\partial t)^*$, $(\partial p/\partial t)^*$, where the coefficients depend on V^*, V_r, and $(\partial V/\partial \xi)_r$. This leads to

THEOREM 5.1. *Suppose that the resolution of the discontinuity at $\xi = 0$, $t = 0$, is as displayed in Fig. 3. Then the time derivatives in the direction of the contact discontinuity $(\partial u/\partial t)^*$, $(\partial p/\partial t)^*$, are determined by a pair of linear equations,*

$$a_r \left(\frac{\partial u}{\partial t}\right)^* + b_r \left(\frac{\partial p}{\partial t}\right)^* = d_r, \tag{5.2}$$

$$a_l \left(\frac{\partial u}{\partial t}\right)^* + b_l \left(\frac{\partial p}{\partial t}\right)^* = d_l. \tag{5.3}$$

The coefficients a_r, b_r, d_r depend on V^*, V_r, $(\partial V/\partial \xi)_r$. The coefficients a_l, b_l, d_l depend on $V^*, V_l, (\partial V/\partial \xi)_l$ and are given by

$$a_l = 1, \qquad b_l = (g_l^*)^{-1}, \qquad d_l = -(g_l g_l^*)^{1/2} a(\beta^*), \tag{5.4}$$

where $\beta^* = g_l^*/g_l$ and $a(\beta)$ is the solution of (4.4).

In the case of a γ-law equation of state explicit formulae for a_r, b_r, d_r are

$$a_r = -(2 + A(p^* - p_r)), \tag{5.5$_\gamma$}$$

$$b_r = A(u^* - u_r) + (g_r^*)^{-2} W_r + W_r^{-1}, \tag{5.6$_\gamma$}$$

$$d_r = L_u \left(\frac{\partial u}{\partial \xi}\right)_r + L_p \left(\frac{\partial p}{\partial \xi}\right)_r + L_\rho \left(\frac{\partial \rho}{\partial \xi}\right)_r, \tag{5.7$_\gamma$}$$

where $W_r = (p^* - p_r)/(u^* - u_r)$ and with $\mu^2 = (\gamma - 1)/(\gamma + 1)$,

$$\begin{aligned} A &= -\tfrac{1}{2}(p^* + \mu^2 p_r)^{-1}, \qquad B = (p^* - p_r)^{-1} - \mu^2 A, \\ L_u &= \rho_r (u_r - u^*)(\gamma p_r B + \tfrac{1}{2}) - W_r, \\ L_\rho &= (2\rho_r)^{-1}(p^* - p_r), \qquad L_p = 1 + B(p^* - p_r). \end{aligned} \tag{5.8$_\gamma$}$$

Proof. Equation (5.2) and the remarks concerning the dependence of a_r, b_r, d_r follow from the considerations preceding the theorem.

To establish (5.3), (5.4) we note that the flow in the region $\xi(\alpha, \beta^*) \leqslant \xi \leqslant 0$ (see Fig. 3 and Sect. 4) is continuously differentiable. Using the chain rule to differentiate along the tail characteristic $\beta = \beta^*$ at $\alpha = 0$ we get

$$\frac{\partial p(0, \beta^*)}{\partial \alpha} = \left(\frac{\partial p}{\partial t}\right)^* \frac{\partial t(0, \beta^*)}{\partial \alpha} + \left(\frac{\partial p}{\partial \xi}\right)_l^* \frac{\partial \xi(0, \beta^*)}{\partial \alpha}. \tag{5.9}$$

From Eq. (1.2) we have that $(\partial p/\partial \xi)_l^* = -(\partial u/\partial t)^*$. Using Eqs. (4.3) and (4.18) the last equation yields

$$g_l \beta^* a(\beta^*) = -g_l^{-1}(\beta^*)^{-1/2}\left(\frac{\partial p}{\partial t}\right)^* - (\beta^*)^{1/2}\left(\frac{\partial u}{\partial t}\right)^*,$$

which is immediately seen to be equivalent to (5.3), (5.4). As was mentioned earlier we discuss in Appendix A the connection betwen (5.3), (5.4) and van Leer's equations.

Finally, to derive Eqs. (5.5_γ)–(5.8_γ) we note that for the γ-law relation the $(p-u)$ Hugoniot is given by (see [5, Sect. 81])

$$K(u, p, u_+, p_+, \rho_+) = u - u_+ - (p - p_+)\left|\frac{1-\mu^2}{\rho_+(p+\mu^2 p_+)}\right|^{1/2}.$$

Carrying out the computations implied by (5.1) and the subsequent considerations yields the desired equations. This concludes the proof.

Remark. Cases other than the one shown in Fig. 3 are dealt with in exactly the same way. The result is always a pair of equations of the form (5.2), (5.3), with the coefficients suitably changed. For the reader's convenience we provide the expressions needed in these cases in Appendix C.

The Case of Weak Waves

In the case of an infinitely weak shock we have $V^* \to V_r$, $W_r \to g_r$ and from Eqs. (5.5_γ)–(5.8_γ), we get then

$$a_r = -2, \qquad b_r = 2g_r^{-1}, \qquad d_r = 2\left(-g_r\left(\frac{\partial u}{\partial \xi}\right)_r + \left(\frac{\partial p}{\partial \xi}\right)_r\right).$$

Similarly, in the case of an infinitely weak rarefaction wave, setting $\beta^* = 1$ in (5.4) and noting (4.5) we get

$$a_l = 1, \qquad b_l = g_l^{-1}, \qquad d_l = -g_l\left(\frac{\partial u}{\partial \xi}\right)_l - \left(\frac{\partial p}{\partial \xi}\right)_l,$$

and the two sets of coefficients are seen to be equivalent, thus rendering consistency of our equations for "sound waves" (notice that since (5.2), (5.3) represent waves propagating in opposite directions, one must substitute r for l, $-u$ for u, and $-\xi$ for ξ in (5.3) and in the expressions for the coefficients in order to obtain equality).

6. The Lagrangian Scheme

Combining the results of Section 5 with the outline in Section 2 we see that there is very little left to complete the description of the Lagrangian scheme. Indeed, the time derivative of the flux vector $\Psi(V)$ (Eq. (1.2)) is given by

$$\left(\frac{\partial \Psi(V)}{\partial t}\right)^n_{i+1/2} = \begin{pmatrix} -\left(\frac{\partial u}{\partial t}\right)^n_{i+1/2} \\ \left(\frac{\partial p}{\partial t}\right)^n_{i+1/2} \\ p^n_{i+1/2}\left(\frac{\partial u}{\partial t}\right)^n_{i+1/2} + u^n_{i+1/2}\left(\frac{\partial p}{\partial t}\right)^n_{i+1/2} \end{pmatrix}, \tag{6.1}$$

(notation as in Section 2), and the derivatives in the right-hand side are furnished by the results of Section 5 (i.e., $(\partial u/\partial t)^*$, $(\partial p/\partial t)^*$). Thus (the Lagrangian equivalent of) Step B of Section 2 is easily implemented (see Appendix C for the coefficients of (5.2), (5.3) in all Lagrangian cases).

Perhaps one final remark is due. When implementing Step D of Section 2, that is, updating planes, we must determine $(\partial \rho/\partial t)^n$, which is of course [illegible]

($\zeta = 0$ is a streamline!)

$$\left(\frac{\partial \rho}{\partial t}\right)^*_r = (c^*_r)^{-2}\left(\frac{\partial p}{\partial t}\right)^* \tag{6.2}$$

and, similarly, for the left-hand side.

7. The Eulerian Scheme

Our starting point here is, again, the discussion at the end of Section 2. Thus, we are led again to consider the time evolution of flow variables for the GRP in the neighborhood of a jump discontinuity with linear distributions on both sides. Only that we are now considering the fixed grid line $x = x_{i+1/2}$. Again, the indices (i, n) are suppressed and we shall use the notation set up in Section 3, where, however, x replaces ξ and the discontinuity is located at $x = 0$, $t = 0$. We realize right away that while the Lagrangian wave pattern is always as shown in Fig. 3 (with possible exchange of shocks and rarefaction waves) the situation in the Eulerian framework is more complicated. Thus, the line $x = 0$ may be located to the right or to the left of both waves or in between, on either side of the contact discontinuity. What is even worse, it may be contained in a centered rarefaction wave moving either way (the "sonic case"). We shall therefore use the following device. First, we use $d\xi = \rho\, dx$ to

define a "local" auxiliary Lagrangian coordinate so that $\xi = 0$ at $x = 0$. The slopes of the initial data at the singularity are then given by

$$\left(\frac{\partial Q}{\partial \xi}\right)_l = \rho_l^{-1}\left(\frac{\partial Q}{\partial x}\right)_l, \qquad \left(\frac{\partial Q}{\partial \xi}\right)_r = \rho_r^{-1}\left(\frac{\partial Q}{\partial x}\right)_r. \tag{7.1}$$

Consequently, the problem can be solved locally as a Lagrangian problem, by means of the methods of Section 5. In particular, Eqs. (5.2), (5.3) are solved and $(\partial u/\partial t)^*$, $(\partial p/\partial t)^*$ determined. Next we "identify" the line $x = 0$ within the Lagrangian framework, that is, we let $\xi = \xi(t)$ be its image under the local transformation $(x, t) \to (\xi, t)$. It is easily verified that $\xi(t)$ satisfies the ordinary differential equation

$$\frac{d\xi}{dt} = -\rho u(\xi, t), \qquad \xi(0) = 0. \tag{7.2}$$

Indeed, we have $x(\xi(t), t) = 0$, hence, by differentiation, $u(\xi(t), t) + (\partial x/\partial \xi)\, \xi'(t) = 0$ and $\partial x/\partial \xi = \rho^{-1}$, by definition. Still we have to determine the value of the right-hand side of (7.2) at 0. This is done in view of our basic hypothesis (1.7). Thus, denoting $U_0 = \lim_{t \to 0} U(0, t)$, we have

$$U_0 = R(0; U_r, U_l), \tag{7.3}$$

where R is now the solution to the RP in *Eulerian coordinates*. The corresponding value of any particular flow variable Q will be denoted by Q_0. (These are the values denoted by $Q^n_{i+1/2}$ in Sect. 2, see (2.2).) Similarly, the time derivative along $x = 0$ is denoted by $(\partial Q/\partial t)_0$. This is the derivative we need in the implementation of Step B of Section 2. Using (7.2) and displaying explicitly the independent variables, one might use the chain rule to obtain

$$\left(\frac{\partial Q}{\partial t}\right)_0 \equiv \frac{\partial}{\partial t} Q(x, t)_{\substack{x=0\cdot \\ t=0}} = \frac{\partial}{\partial t} Q(\xi, t)_{t=0} - \rho_0 u_0 \frac{\partial}{\partial \xi} Q(\xi, t)_{t=0}. \tag{7.4}$$

Observe that both derivatives in the right-hand side of (7.4) are evaluated at $\xi = \xi(t)$ and then $t \to 0$. Unfortunately, Eq. (7.4) is not always meaningful. More specifically, in the sonic case the ξ derivative in the right-hand side generally blows up as the singularity is approached. In this case we shall find it necessary to use characteristic coordinates and modify (7.4) accordingly.

Consider Fig. 3 again, where now ξ is the local Lagrangian coordinate. We number from $k = 1$ to 6 the zones determined by the waves, including the waves themselves, apart from the contact discontinuity which is always the curve $\xi = 0$. In what follows we assume that the wave configuration is as shown in Fig. 3 and let $W_e = \rho_r^{-1} W_r + u_r$ be the Eulerian shock speed $(W_r = (p^* - p_r)/(u^* - u_r))$. Recall that U^* is the solution of the RP along the contact discontinuity. We may now classify the various possibilities for the location of $\xi = \xi(t)$.

A. *The Nonsonic Case.* Here Eq. (7.4) is meaningful where, with $\xi(t)$ located in zone k:

(a) $k=1$ if $u_l - c_l > 0$, then $U_0 = U_l$.

(b) $k=3$ if $u^* - c_l^* < 0 < u^*$, then $U_0 = U_l^*$.

(c) $k=4$ if $u^* < 0 < W_e$, then $U_0 = U_r^*$.

(d) $k=6$ if $W_e < 0$, then $U_0 = U_r$.

B. *The Sonic Case.* Here Eq. (7.4) is meaningless. The curve $\xi = \xi(t)$ is contained in a rarefaction fan and by (7.3) U_0 is determined as the value carried by the sonic line. In the case shown in Fig. 3 we have

$$k=2 \qquad \text{if} \quad u_l - c_l \leqslant 0 \leqslant u^* - c_l^*.$$

Observe that the classification is made solely on the basis of the Riemann solver $R(\cdot; U_r, U_l)$. We shall now discuss the two cases separately.

A. *The Nonsonic Case*

Let the "zone index" be k as above. For all four possibilities we need to interpret the derivatives in the right-hand side of (7.4). Unlike the Lagrangian case (Sect. 6) where essentially we needed time derivatives for u, p only (and (6.2)), it follows from (1.1) that in the Eulerian case we need the derivatives for all basic variables, that is, ρ, p, u. Let us examine the various possibilities.

(a) $k=1$. In (7.4) we use, in accordance with (1.2),

$$\begin{aligned} &\frac{\partial}{\partial \xi} Q(\xi, t)_{t=0} = \left(\frac{\partial Q}{\partial \xi}\right)_l \qquad \text{(as given by (7.1))}, \\ &\frac{\partial}{\partial t} V(\xi, t)_{t=0} = -\Psi'(V_l)\left(\frac{\partial V}{\partial \xi}\right)_l. \end{aligned} \tag{7.5}$$

Since p is not explicitly included as a component of V, the equality $(\partial/\partial t)\, p(\xi, t)_{t=0} = c_l^2 (\partial/\partial t)\, \rho(\xi, t)_{t=0}$ may be used.

(b) $k=6$. This case is completely analogous to the case $k=1$, with l replaced by r.

(c) The cases $k=3, 4$. Here the time derivatives are easy to compute. Indeed if $Q = u$ or p then

$$\frac{\partial}{\partial t} Q(\xi, t)_{t=0} = \left(\frac{\partial Q}{\partial t}\right)^*, \tag{7.6}$$

and for ρ we use (6.2). Thus, the results of Section 5 are applicable here. Consider now the ξ derivative in (7.4). Using the notation of Table I (Sect. 3), these are precisely $(\partial Q/\partial \xi)_l^*$ $(k=3)$ or $(\partial Q/\partial \xi)_r^*$ $(k=4)$. In view of (1.2), this is easy for $Q = u, p$. Indeed,

$$\left(\frac{\partial u}{\partial \xi}\right)_l^* = -(\rho_l^*)^{-2}\left(\frac{\partial \rho}{\partial t}\right)_l^* = -(g_l^*)^{-2}\left(\frac{\partial p}{\partial t}\right)^*,$$
$$\left(\frac{\partial p}{\partial \xi}\right)_l^* = -\left(\frac{\partial u}{\partial t}\right)^*, \tag{7.7}$$

with analogous formulae for $k = 4$. These derivatives, therefore, follow from the results of Section 5. It remains to compute $(\partial\rho/\partial\xi)_r^*$, $(\partial\rho/\partial\xi)_l^*$. We shall do that in Theorem 7.1, in which we summarize the results for the nonsonic cases.

THEOREM 7.1 (Nonsonic case). *Let the line $x = x_{i+1/2}$ be nonsonic and suppose that the configuration is as shown in Fig. 3 (where $x_{i+1/2} = 0$). Then in order to implement Step* B *of Section 2 for the Eulerian case one uses Eq. (7.4) supplemented as follows*:

(i) *If $k = 1$ or $k = 6$, Eqs. (7.5) are used (r for l when $k = 6$).*

(ii) *If $k = 3, 4$, the interface derivatives $(\partial u/\partial t)^*$, $(\partial p/\partial t)^*$ are evaluated as in Section 5. Then Eqs. (7.6), (6.2), (7.7) are used for all but the ξ derivatives of ρ, which are computed as follows: Let $\partial\rho(0,\beta)/\partial\alpha$ be given by (4.21) and $\beta^* = g_l^*/g_l$ at the tail of rarefaction. Then,*

$$\left(\frac{\partial \rho}{\partial \xi}\right)_l^* = (\beta^*)^{-1/2}\frac{\partial \rho(0,\beta^*)}{\partial \alpha} + (g_l^*)^{-1}(c_l^*)^{-2}\left(\frac{\partial p}{\partial t}\right)^*, \tag{7.8}$$

$$\begin{aligned}\left(\frac{\partial \rho}{\partial \xi}\right)_r^* &= 3(\rho_r^*)^2 W_r^{-2}\left(\frac{\partial u}{\partial t}\right)^* - (3(c_r^*)^{-2}W_r^{-1} + (\rho_r^*)^2 W_r^{-3})\left(\frac{\partial p}{\partial t}\right)^* \\ &\quad - (3 + g_r^2 W_r^{-2})(\rho_r^*)^2 W_r^{-1}\left(\frac{\partial u}{\partial \xi}\right)_r \\ &\quad + 3(\rho_r^*)^2 W_r^{-2}\left(\frac{\partial p}{\partial \xi}\right)_r + (\rho_r^*)^2 \rho_r^{-2}\left(\frac{\partial \rho}{\partial \xi}\right)_r,\end{aligned} \tag{7.9}$$

where $W_r = (p^* - p_r)/(u^* - u_r)$, $g_r = \rho_r c_r$.

Proof. In view of the foregoing remarks we need to prove only (7.8), (7.9). To establish (7.8) we proceed as in (5.9) to obtain

$$\frac{\partial \rho(0,\beta^*)}{\partial \alpha} = (c_l^*)^{-2}\left(\frac{\partial p}{\partial t}\right)^* \frac{\partial t(0,\beta^*)}{\partial \alpha} + \left(\frac{\partial \rho}{\partial \xi}\right)_l^* \frac{\partial \xi(0,\beta^*)}{\partial \alpha}.$$

To prove (7.9) we use a procedure similar to (5.1). Specifically, using a well-known shock relation [5, Eq. (59.05)] and the same notation as in (5.1) we have

$$\left(\frac{\partial}{\partial t} + W\frac{\partial}{\partial \xi}\right)\left[(p - p_+)\left(\frac{1}{\rho_+} - \frac{1}{\rho}\right) - (u - u_+)^2\right] = 0. \tag{7.10}$$

The preshock time derivatives are transformed into spatial derivatives and the postshock derivatives $\partial p/\partial \xi$, $\partial u/\partial \xi$ are transformed into time derivatives as indicated in the paragraph following (5.1). We note that $\partial p/\partial t = c^{-2}(\partial p/\partial t)$. Solving the last equation for $\partial p/\partial \xi$, using that $W_r(\rho_r^{-1} - (\rho_r^*)^{-1}) = u^* - u_r$ and letting $t \to 0$ we get (7.9). This concludes the proof of the theorem.

Theorem 7.1 allows one to use Eq. (7.4) in the nonsonic cases. In Appendix D we give the analogues of (7.8), (7.9) for the cases that a rarefaction wave is travelling to the right or a shock is travelling to the left.

B. *The Sonic Case*

Here we use the same "local" Lagrangian coordinates as before, leading to the trajectory (7.2) as the image of $x = 0$, with U_0 as given by (7.3). However, Eq. (7.4) is replaced as follows:

We assume that the configuration is as shown in Fig. 3, hence $k = 2$ in our case. Let (α, β) be the characteristic coordinates as defined in Section 4. The line $x = 0$ is sonic, namely, $u_0 = c_0$. Let $\beta_0 = g_0/g_l$, where $g_0 = \rho_0 c_0 = \rho_0 u_0$. By (4.1) the characteristic $\beta = \beta_0$ coincides with $x = 0$ for the solution of the "associated Riemann problem." Let $(\alpha(t), \beta(t))$ be the representation of $x = 0$, so that $(\alpha(0), \beta(0)) = (0, \beta_0)$. In general, this curve is not tangent to the characteristic $\beta = \beta_0$ in the (α, β) plane, that is, $\beta'(0) \neq 0$, even though they are tangent in the (ξ, t) plane (you might think of a curve $r(\lambda)$, $\theta(\lambda)$ in polar coordinates, with $\theta'(0) \neq 0$). Instead of Eq. (7.4) we shall use, in this case,

$$\left(\frac{\partial Q}{\partial t}\right)_0 = \frac{\partial}{\partial t} Q(x, t)_{\substack{x=0 \\ t=0}} = \frac{\partial}{\partial \alpha} Q(0, \beta_0)\, \alpha'(0) + \frac{\partial}{\partial \beta} Q(0, \beta_0) \cdot \beta'(0). \tag{7.11}$$

As in Section 4, all quantities are smooth functions of (α, β) up to the singularity $\alpha = 0$. The value of β_0 (when $k = 2$) is determined by

$$u(0, \beta_0) = c(0, \beta_0). \tag{7.12}$$

Thus β_0, as well as all the functions $Q(0, \beta)$, are determined by the solution to the "associated Riemann problem." For a γ-law relation these functions are given in (4.16_γ), whereas from (7.12) we infer that

$$\beta_0 = \left[\frac{\gamma - 1}{\gamma + 1}\left(\frac{u_l}{c_l} + \frac{2}{\gamma - 1}\right)\right]^{(\gamma+1)/(\gamma-1)} \qquad (k = 2). \tag{7.13_γ}$$

In view of Theorem 4.1 and Corollary 4.2 the only missing elements in (7.11) are $\alpha'(0)$, $\beta'(0)$. They are given, along with a summary of the previous remarks, in Theorem 7.2.

THEOREM 7.2 (Sonic case). *Let the line $x = x_{i+1/2}$ be sonic and contained in a Γ^--rarefaction fan, as shown in Fig.* 3 *(with $x_{i+1/2} = 0$). Then in order to implement Steps* A–C *of Section* 2 *the following steps are taken:*

(a) *The solution of the "associated Riemann problem" in the expansion wave is determined* ((4.16$_\gamma$) *for a* γ*-law*).

(b) *The characteristic that coincides with the grid line is singled out in terms of its slope* β_0 (*in the "local" Lagrangian representation*), *using* (7.12) ((7.13$_\gamma$) *for a* γ*-law*).

(c) *The initial values* U_0 *in* (7.3) *are determined as* $U(0, \beta_0)$ (*corresponding to* $U^n_{i+1/2}$ *in* (2.2)).

(d) *The time derivatives* $(\partial Q/\partial t)_0$ (*corresponding to* $(\partial U/\partial t)^n_{i+1/2}$ *in Step* B) *are*

$$\alpha'(0) = -g_l \beta_0^{1/2}, \tag{7.14}$$

$$\beta'(0) = \tfrac{1}{2}\beta_0^{1/2}\left[\frac{\partial}{\partial \alpha}(\rho c)(0, \beta_0) - \frac{\partial}{\partial \alpha}(\rho u)(0, \beta_0)\right]. \tag{7.15}$$

(e) *For the flux vector* $\Phi(U)$ *of* (1.1) *we have*

$$\frac{\partial}{\partial \beta}\Phi(0, \beta_0) = 0, \tag{7.16}$$

so that from (7.11),

$$\left(\frac{\partial \Phi(U)}{\partial t}\right)_0 = \frac{\partial}{\partial \alpha}\Phi(0, \beta_0) \cdot \alpha'(0).$$

(See remarks in Appendix D concerning the sonic case for $k = 5$.)

Proof. We need only prove (7.14)–(7.16). Differentiating the second equation in (4.3) with respect to t along $\alpha(t)$, $\beta(t)$ we get

$$1 = \frac{\partial t}{\partial \alpha}\alpha'(t) + \frac{\partial t}{\partial \beta}\beta'(t) = -g_l^{-1}\beta(t)^{-1/2}\alpha'(t) + O(\alpha(t)).$$

Letting $t \to 0$, so that $(\alpha(t), \beta(t)) \to (0, \beta_0)$ we obtain (7.14).

Equation (7.15) is considerably more difficult to prove. We postpone the proof to Appendix B. To prove (7.16) we note that the isentropic Γ^+ relations hold along the degenerate $\alpha = 0$ characteristic, so that

$$\frac{\partial}{\partial \beta}u(0, \beta) + g(0, \beta)^{-1}\frac{\partial}{\partial \beta}p(0, \beta) = 0,$$

$$\frac{\partial}{\partial \beta}u(0, \beta) + \frac{c(0, \beta)}{\rho(0, \beta)}\frac{\partial}{\partial \beta}\rho(0, \beta) = 0.$$

Combining these relations with (7.12) yields (7.16).

Remarks. (1) Note that in view of (7.17), (2.3), and (2.4) the full equation (7.11) (hence, $\beta'(0)$) is needed only if slopes are updated by (2.5), that is, "interface differencing." If another method is used in Step D (e.g., "average differencing," see [2]) then $\beta'(0)$ is immaterial.

(2) Equation (7.15) expresses the "curvature" of the characteristic $\beta = \beta_0$, that is, its deviation from a straight line along which $u - c$ vanishes identically.

Summary

The Eulerian scheme has been completely described in Theorems 7.1 and 7.2. Observe that the "local" Lagrangian coordinates were used only to simplify the characteristic picture. Starting from constant Eulerian slopes on both sides of $x_{i+1/2}$, one defines new slopes as in (7.1), then uses either (7.4) or (7.11) to evaluate the Eulerian time derivatives. As a matter of fact, it follows from our analysis that these time derivatives at $x_{i+1/2}$ depend only on the *limiting values* $\lim_{x \to x_{i+1/2}\pm}(\partial Q/\partial x)$. Thus, in principle, the method can be extended to the case that the slope in cell i is nonconstant.

8. Numerical Examples

We have chosen three one-dimensional examples to illustrate various aspects of our schemes. All three of them have been discussed in the literature recently and served as test problems in the comparison and assessment of a variety of first- and second-order schemes. Before presenting the results let us refer briefly to the question of monotonicity algorithms. As was observed in [2, 3, 11], such algorithms are crucial in the development of upstream-centered second-order schemes. On the other hand, they are still accessory techniques, largely independent of the particular difference scheme used. A basic requirement of these algorithms is, of course, that they serve well and adjust automatically to a large variety of cases, regardless of the particular nature of any one case. Our approach was, therefore, to minimize the role played by the monotonicity algorithms as much as possible, admittedly at the expense of possibly missing the best result sometimes in a given case (this is illustrated in example (b) below). Thus, we updated slopes as in Step D, Section 2 (i.e., updating values at cell boundaries and then taking differences). We then used the basic alforithm of van Leer (see [11, Fig. 3]), which can be summarized by the following principles: (A) If the cell average is an extremum, the slope is set equal to zero. (B) The slope is reduced so that cell-boundary values do not go beyond the cell averages in the neighboring cells.

All three examples shown below were worked out using solely this algorithm.

(a) Our first example is the shock-tube problem used by Sod [10]. The tube extends from $x = 0$ to $x = 100$ and is divided into 100 equal cells. The gas is initially at rest ($u = 0$) with $p = 1$, $\rho = 1$ for $0 \leqslant x < 50$, $p = 0.1$, $\rho = 0.125$ for $50 < x \leqslant 100$. Numerical and exact solutions are shown at $t = 15$, when the shock wave moving to

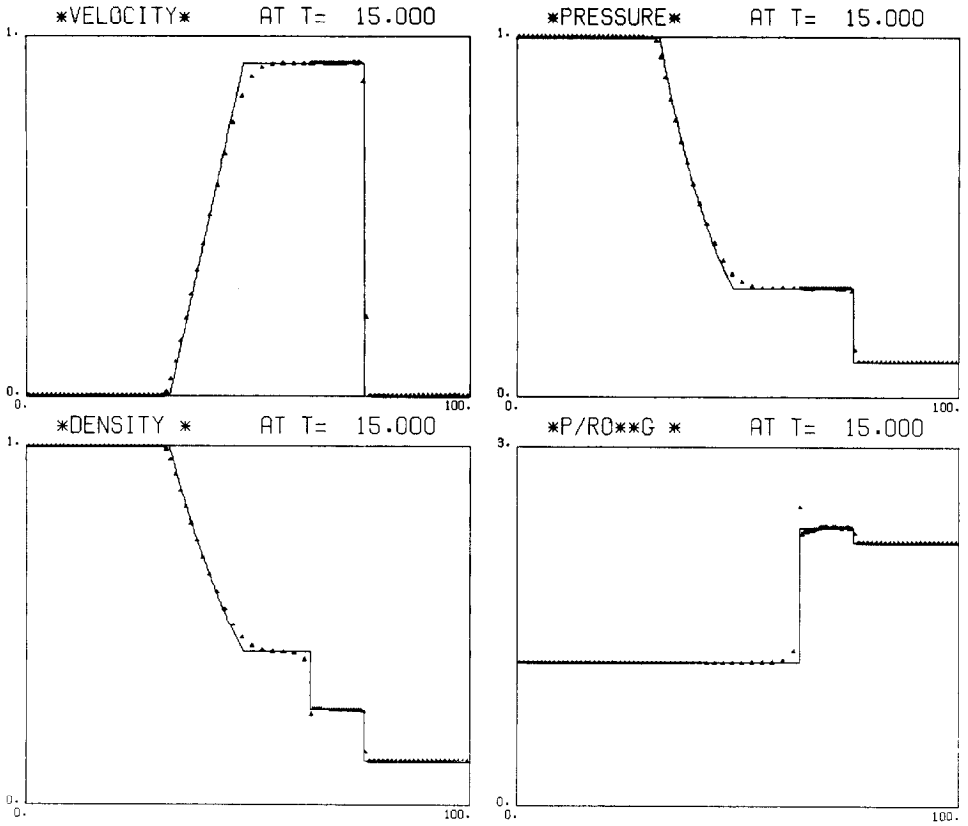

FIG. 4. Results for Sod's problem, using the Lagrangian scheme (see Ex. (a), Sect. 8).

the right has approximately reached $x = 75$. The solid lines represent the exact solutions, whereas the dots represent cell averages in the numerical solution. The quantities shown are velocity, pressure, density, and p/ρ^{γ}, which is a function of entropy (here $\gamma = 1.4$). Figure 4 shows the results of the Lagrangian scheme (Section 6) and Fig. 5 shows the results of the Eulerian scheme (Section 7).

(b) The second example was used by Colella and Woodward in [3] in order to test their piecewise-parabolic method and the associated monotonicity algorithms. It is a Riemann problem which involves a very strong nearly stationary shock wave. The region of integration is again $0 \leqslant x \leqslant 100$ and is divided into 100 equal cells. Initially, $p = \frac{4}{3}$, $\rho = 4$, and $u = -0.3$ for $0 \leqslant x < 20$ and $p = 10^{-6}$, $\rho = 1$, and $u = -1.3$ for $20 < x \leqslant 100$. Transmitting (influx) boundary conditions are applied at the boundaries. The gas is ideal with $\gamma = \frac{5}{3}$, so that the jump in density $((\gamma + 1)/(\gamma - 1))$ represents the limiting value for a jump across a shock. The initial data are so adjusted that the exact solution consists of a single shock moving to the right at a (Eulerian) speed of approximately 0.033. Figure 6 displays the results of

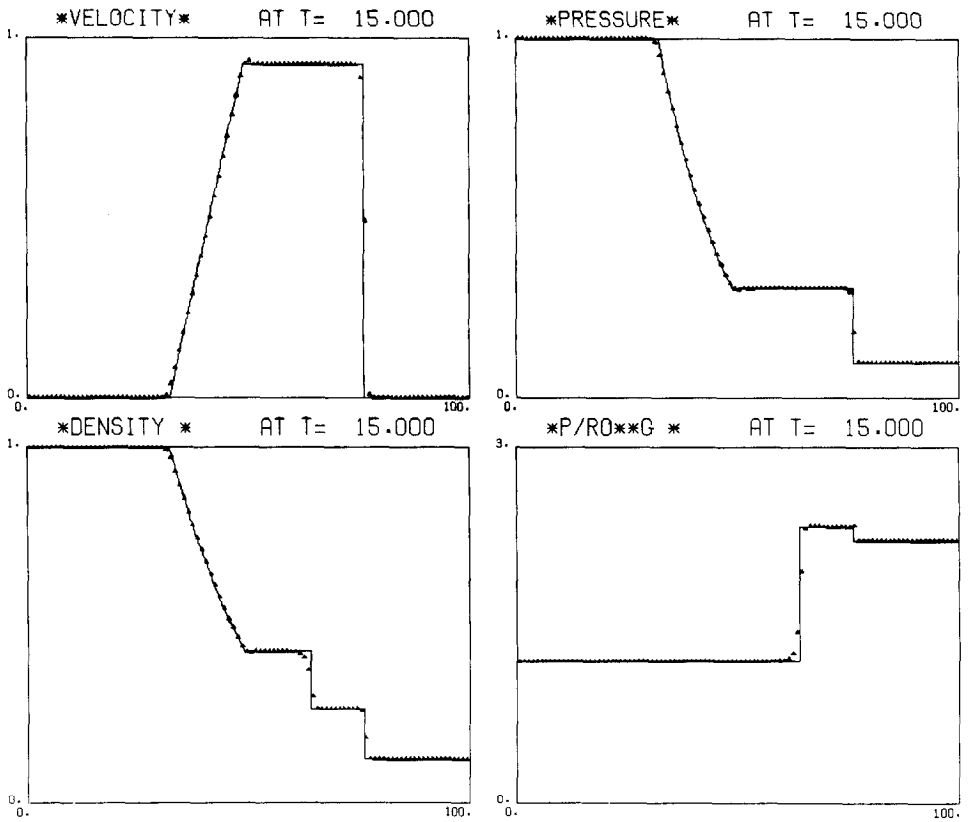

FIG. 5. Results for Sod's problem, using the Eulerian scheme (see Ex. (a), Sect. 8).

the Eulerian scheme at $t = 2000$, after 4000 cycles of a constant $\Delta t = 0.5$. The shock has moved by then about 66 cells. Again the exact and numerical solution are represented, respectively, by the solid lines and dots. For the density profile we get the same "wavelike" behavior as pointed out in [3]. However, the velocity and pressure profiles are quite sharp and also the deviation in entropy is quite moderate. Of course, the profiles can be further smoothed out by enhancing the dissipative mechanism, or, in this case, flattening further the slopes of flow quantities in cells. This is nicely demonstrated in Fig. 7, in which all slopes were set equal to zero, thus obtaining the first-order Godunov–Eulerian scheme (under otherwise identical terms).

(c) Our final example was again proposed by Colella and Woodward in [4]. Unlike the previous two examples, it involves multiple interactions of waves of all kinds. We refer the reader to [4] for a detailed discussion of the various interactions encountered there (after the main feature of the flow they refer to the problem as "two interacting blast waves"). The initial condition consists of three constant states at rest ($u = 0$) between rigid (reflecting) walls located at $x = 0$ and $x = 100$. The

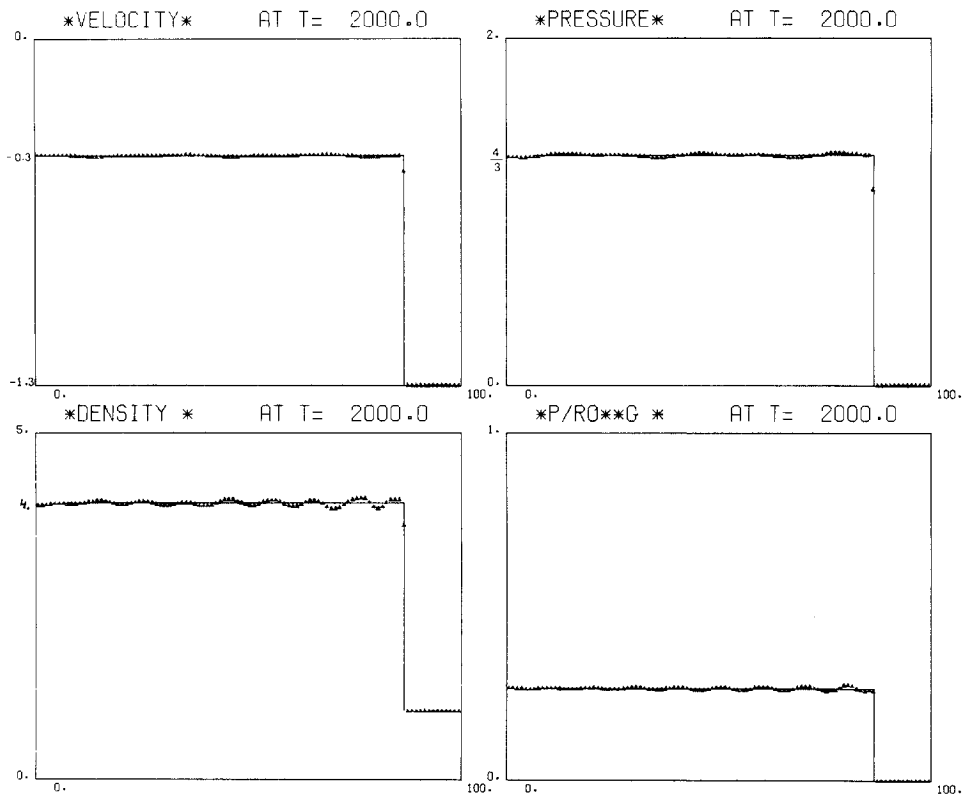

FIG. 6. Numerical and exact solution for a very strong almost stationary shock (see Ex. (b), Sect. 8), using the Eulerian scheme.

density is everywhere unity, while the pressure is 1000 for $0 \leqslant x < 10$ and 100 for $90 < x \leqslant 100$, while it is only 0.01 in $10 < x < 90$. The gas is ideal with $\gamma = 1.4$. Following [4], we use the velocity and density profiles at $t = 3.8$ as a basis for comparison. Figure 8 displays our numerical results using the Eulerian scheme. In Fig. 8a we used 200 equal cells, while in Fig. 8b we used 800 equal cells. Comparing our results with the most accurate run in [4] (using 2400 cells) we see that the solution in Fig. 8b is quite accurate, except for some smearing of contact discontinuities. We note that our solution is very close to the MUSCL solution (using 1200 cells), as displayed in [4].

APPENDIX A: RELATION TO VAN LEER'S EQUATION FOR A CENTERED RAREFACTION WAVE

At the end of Section 5 we considered the case of an infinitely weak rarefaction wave, that is, $\beta^* = 1$. In a region of smooth flow this corresponds to an error of the

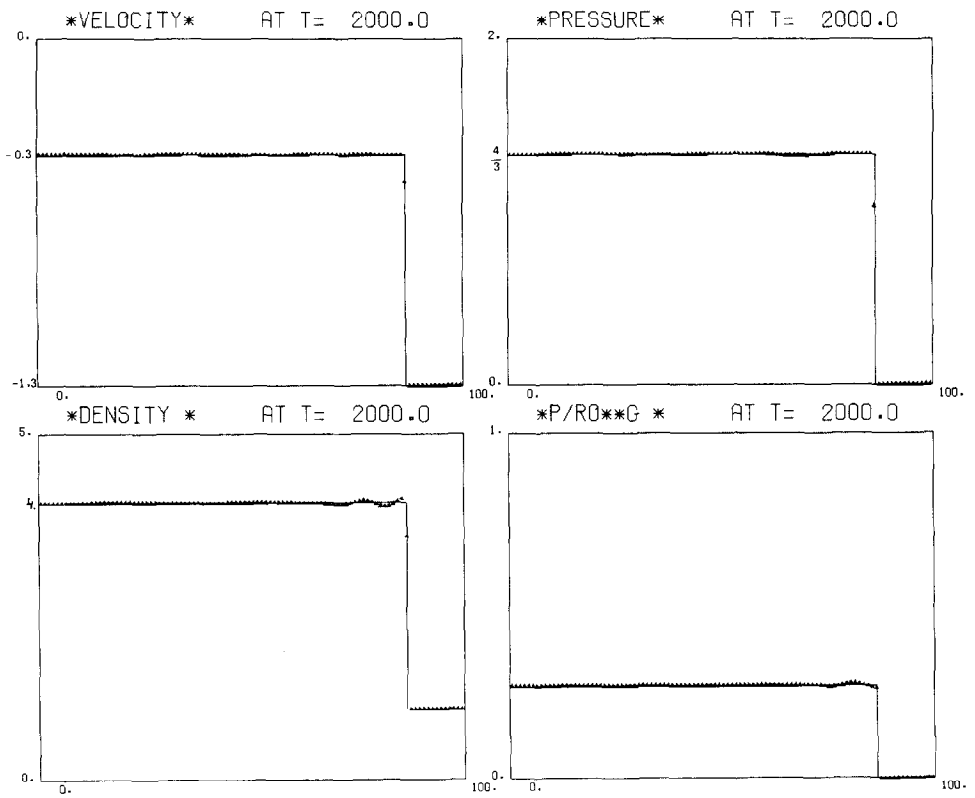

FIG. 7. Numerical and exact solution for a very strong almost stationary shock (see Ex. (b), Sect. 8), using Godunov's first-order Eulerian scheme.

order $O(\Delta x)$ in the coefficients of (5.3) (specifically d_l, see (5.4)). We now go one step further and study the approximation of d_l to within $O(\Delta x^2)$. In other words, we expand d_l up to linear terms in $\beta^* - 1 = (g_l^* - g_l)/g_l$. We shall do that for the γ-law relation, where $a(\beta)$ is given by (4.7_γ). So, omitting higher order terms and using equality to mean "within $O(\Delta x^2)$" we get

$$a(\beta^*) = \left(\frac{\partial u}{\partial \xi}\right)_l + g_l^{-1}\left(\frac{\partial p}{\partial \xi}\right)_l + g_l^{-1}(\gamma+1)^{-1}\left[c_l\left(\frac{\partial g}{\partial \xi}\right)_l - \frac{\gamma+1}{2}\left(\frac{\partial p}{\partial \xi}\right)_l\right]\cdot\frac{g_l^* - g_l}{g_l}. \tag{A.1}$$

Recall that $g = (\gamma p \rho)^{1/2}$, hence,

$$\left(\frac{\partial g}{\partial \xi}\right)_l = \frac{1}{2g_l}\left(\frac{\partial}{\partial \xi} g^2\right)_l = \frac{\gamma}{2g_l}\left(p_l\left(\frac{\partial \rho}{\partial \xi}\right)_l + \rho_l\left(\frac{\partial p}{\partial \xi}\right)_l\right),$$

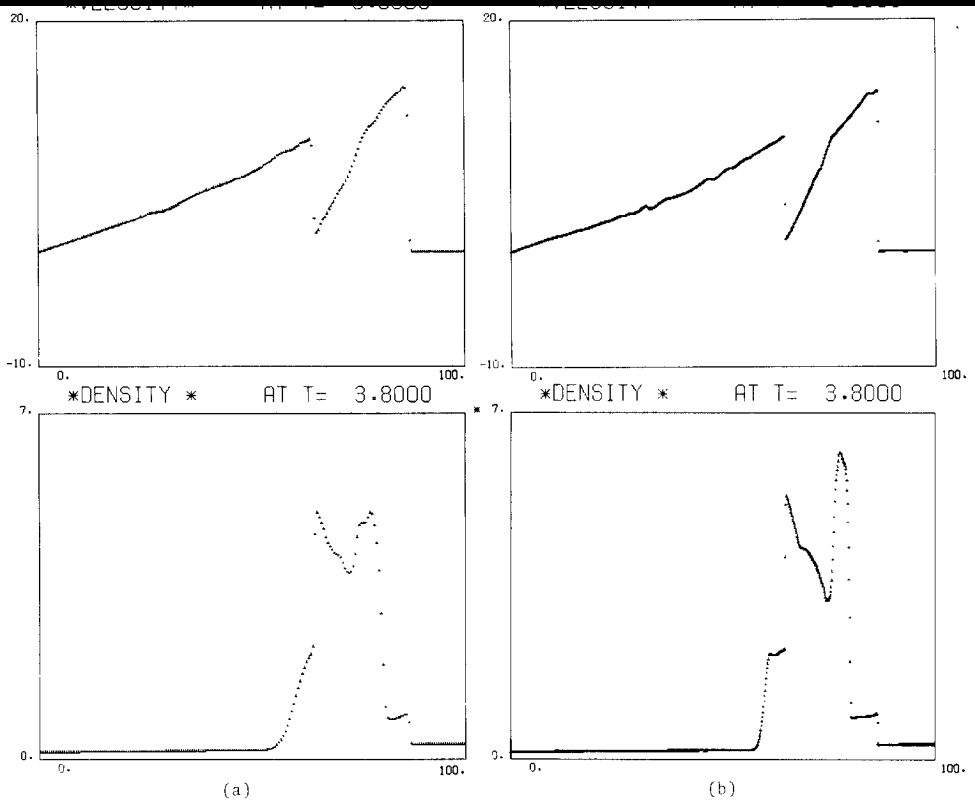

FIG. 8. Numerical results for two interacting blast waves (Ex. (c), Sect. 8), using the Eulerian scheme, (a) with 200 cells, (b) with 800 cells.

so that

$$c_l\left(\frac{\partial g}{\partial \xi}\right)_l - \frac{\gamma+1}{2}\left(\frac{\partial p}{\partial \xi}\right)_l = \frac{1}{2}c_l^2\left(\frac{\partial \rho}{\partial \xi}\right)_l - \frac{1}{2}\left(\frac{\partial p}{\partial \xi}\right)_l. \tag{A.2}$$

Let $\Delta p = p^* - p_l$, $\Delta \rho = \rho_l^* - \rho_l$, $\Delta g = g_l^* - g_l$, and set $W = \frac{1}{2}(g_l^* + g_l)$. Since $\rho_l \Delta p = \gamma p_l \Delta \rho$ we have

$$2W \cdot \Delta g = \Delta(g^2) = \gamma \Delta(p\rho) = \gamma(\gamma+1)\, p_l \Delta \rho.$$

Since $W = g_l + \frac{1}{2}\Delta g$, we have, again within $O(\Delta x^2)$,

$$\frac{\Delta g}{g_l^2(\gamma+1)} = \frac{\Delta \rho}{2W\rho_l} = \rho_l \frac{\Delta \tau}{2W} \qquad \left(\tau = \frac{1}{\rho}\right). \tag{A.3}$$

Inserting (A.2), (A.3) into (A.1) yields

$$a(\beta^*) = \left(\frac{\partial u}{\partial \xi}\right)_l + g_l^{-1}\left(\frac{\partial p}{\partial \xi}\right)_l + (4W\tau_l)^{-1}\left(\left(\frac{\partial p}{\partial \xi}\right)_l + g_l^2\left(\frac{\partial \tau}{\partial \xi}\right)_l\right)\Delta\tau.$$

Within the required order of accuracy $W^2 = g_l\, g_l^*$, so from (5.4) we finally get

$$d_l = -W\left(\left(\frac{\partial u}{\partial \xi}\right)_l + g_l^{-1}\left(\frac{\partial p}{\partial \xi}\right)_l\right) - (4\tau_l)^{-1}\left(\left(\frac{\partial p}{\partial \xi}\right)_l + g_l^2\left(\frac{\partial \tau}{\partial \xi}\right)_l\right)\Delta\tau.$$

This is exactly the coefficient used by van Leer [11, Eq. (65)].

APPENDIX B: The Sonic Case

In this appendix we prove Eq. (7.15) and then discuss briefly the equivalents of Eqs. (7.11), (7.12), (7.13$_\gamma$) for a Γ^+-rarefaction wave ($k = 5$).

Proof of (7.15). Since $\alpha = \text{const.}$, $\beta = \text{const.}$ are Γ^+, Γ^- characteristics, respectively, we have

$$\frac{\partial \xi}{\partial \alpha} = -g\frac{\partial t}{\partial \alpha}, \tag{B.1}$$

$$\frac{\partial \xi}{\partial \beta} = g\frac{\partial t}{\partial \beta}. \tag{B.2}$$

Using (4.3) in (B.1) and dropping all terms which are $O(\alpha^2)$, we obtain

$$\begin{aligned}\beta^{1/2} + 2\alpha\varepsilon(0,\beta) &= -g(0,\beta)[-g_l^{-1}\beta^{-1/2} + 2\alpha\eta(0,\beta)] + g_\alpha(0,\beta)\, g_l^{-1}\beta^{-1/2}\alpha \\ &= \beta^{1/2} + g_\alpha(0,\beta)\, g_l^{-1}\beta^{-1/2}\alpha - 2g_l\beta\eta(0,\beta)\alpha,\end{aligned}$$

where (4.15) was used. Rearranging the last equation we get

$$\varepsilon(0,\beta) = \tfrac{1}{2} g_\alpha(0,\beta)\, g_l^{-1}\beta^{-1/2} - g_l\beta\eta(0,\beta). \tag{B.3}$$

Similarly, using (4.3) in (B.2) and dropping all terms which are $O(\alpha^3)$ yields

$$\begin{aligned}\tfrac{1}{2}\alpha\beta^{-1/2} + \varepsilon_\beta(0,\beta)\alpha^2 = g(0,\beta)[&\tfrac{1}{2} g_l^{-1}\alpha\beta^{-3/2} + \eta_\beta(0,\beta)\alpha^2] \\ &+ \tfrac{1}{2} g_\alpha(0,\beta)\, g_l^{-1}\alpha^2\beta^{-3/2},\end{aligned}$$

which reduces to

$$\varepsilon_\beta(0,\beta) = g_l\beta\eta_\beta(0,\beta) + \tfrac{1}{2} g_l^{-1} g_\alpha(0,\beta)\beta^{-3/2}. \tag{B.4}$$

Equations (B.3), (B.4) are a pair of ordinary differential equations for $\varepsilon(0,\beta)$, $\eta(0,\beta)$.

Differentiating (B.3) with respect to β and eliminating $\eta(0, \beta)$ we get

$$\frac{d}{d\beta}(\beta^{-1/2}\varepsilon(0, \beta)) = \frac{1}{4} g_l^{-1}\beta^{-1/2} \frac{d}{d\beta}(\beta^{-1/2} g_\alpha(0, \beta)). \tag{B.5}$$

Our choice of the characteristic $\beta = 1$ was such (see the paragraph following (4.2)) that $\xi(\alpha, 1) = \alpha$, hence,

$$\varepsilon(0, 1) = 0, \tag{B.6}$$

which constitutes the initial condition needed in (B.5). Note that $g_\alpha(0, \beta)$ is given by (4.19), (4.20$_\gamma$). Having solved for $\varepsilon(0, \beta)$, we determine $\eta(0, \beta)$ from (B.3).

To proceed with the proof of (7.15), let $\alpha(t)$, $\beta(t)$ be the characteristic representation of $x = 0$, and let $\xi(t)$ be its representation by (7.2). Differentiating along $\xi(t)$ we get

$$\frac{d\xi}{dt} = \frac{\partial \xi}{\partial \alpha}\alpha'(t) + \frac{\partial \xi}{\partial \beta}\beta'(t) = (\beta^{1/2} + 2\alpha\varepsilon(\alpha, \beta))\,\alpha'(t) + \tfrac{1}{2}\alpha\beta^{-1/2}\beta'(t) + O(\alpha^2).$$

On the other hand, by (7.2),

$$\begin{aligned}\frac{d\xi}{dt} &= -\rho u(\alpha(t), \beta(t)) \\ &= -\rho u(0, \beta_0) - \frac{\partial}{\partial \alpha}(\rho u)(0, \beta_0)\,\alpha(t) - \frac{\partial}{\partial \beta}(\rho u)(0, \beta_0)(\beta(t) - \beta_0) + O(t^2).\end{aligned}$$

From (7.16) we infer that $(\partial/\partial\beta)\,\rho u(0, \beta_0) = 0$. Equating zero order terms in the last two expressions and using (7.12) we recover (7.14). For first order terms we have

$$\begin{aligned}&\alpha'(0)\,\beta_0^{-1/2}\beta'(0) + \beta_0^{1/2}\alpha''(0) \\ &\quad = -2\alpha'(0)^2\varepsilon(0, \beta_0) - \frac{\partial}{\partial \alpha}(\rho u)(0, \beta_0)\,\alpha'(0).\end{aligned} \tag{B.7}$$

Similarly, we have from (4.3) that

$$\begin{aligned}1 = \frac{dt}{dt} &= (-g_l^{-1}\beta^{-1/2} + 2\alpha\eta(\alpha, \beta))\,\alpha'(t) + \tfrac{1}{2} g_l^{-1}\alpha\beta^{-3/2}\beta'(t) + O(\alpha^2) \\ &= g_l^{-1}\{-\beta_0^{-1/2}\alpha'(0) \\ &\quad + [(\beta_0^{-3/2}\beta'(0) + 2g_l\alpha'(0)\,\eta(0, \beta_0))\,\alpha'(0) - \beta_0^{-1/2}\alpha''(0)]t\} + O(t^2),\end{aligned}$$

whence,

$$\alpha'(0)\,\beta_0^{-3/2}\beta'(0) - \beta_0^{-1/2}\alpha''(0) = -2g_l\alpha'(0)^2\eta(0, \beta_0). \tag{B.8}$$

Multiplying (B.8) by β_0, adding to (B.7), and taking (B.3) into account, we get

$$2\beta_0^{-1/2}\beta'(0) = -g_l^{-1}\alpha'(0)\beta_0^{-1/2}\frac{\partial}{\partial\alpha}g(0,\beta_0) - \beta_0\frac{\partial}{\partial\alpha}(\rho u)(0,\beta_0)$$

and, finally, using (7.14),

$$\beta'(0) = \frac{1}{2}\beta_0^{1/2}\left[\frac{\partial}{\partial\alpha}g(0,\beta) - \frac{\partial}{\partial\alpha}(\rho u)(0,\beta_0)\right],$$

which is (7.15).

Remarks on the Sonic Case for a Γ^+ Rarefaction

We define characteristic coordinates (α,β) as in Section 4, except that now $\alpha = \text{const.}$, $\beta = \text{const.}$ are Γ^-, Γ^+ curves, respectively. The coordinate β is the normalized slope of the Γ^+ characteristics fanning out from the origin. Instead of (7.12), the sonic line is now given by $u(0,\beta_0) = -c(0,\beta_0)$. If we reflect $(u,\xi,\alpha)\to(-u,-\xi,-\alpha)$, $(p,\rho,g,\beta)\to(p,\rho,g,\beta)$ and change r to l, we obtain precisely the $k=2$ case. Thus, instead of (7.13_γ) we have

$$\beta_0 = \left|\frac{\gamma-1}{\gamma+1}\left(-\frac{u_r}{c_r}+\frac{2}{\gamma-1}\right)\right|^{(\gamma+1)/(\gamma-1)} \qquad (k=5) \qquad (B.9_\gamma)$$

and instead of (7.14), (7.15) we get

$$\alpha'(0) = g_r\beta_0^{1/2}, \tag{B.10}$$

$$\beta'(0) = -\frac{1}{2}\beta_0^{1/2}\left[\frac{\partial}{\partial\alpha}(\rho c)(0,\beta_0) + \frac{\partial}{\partial\alpha}(\rho u)(0,\beta_0)\right]. \tag{B.11}$$

It is equally easy to see how the equations in Corollary 4.2 change under the above transformations. Particularly, the expression (4.7_γ) transforms into

$$a(\beta) = \left(\frac{\partial u}{\partial\xi}\right)_r - g_r^{-1}\left(\frac{\partial p}{\partial\xi}\right)_r + \frac{2}{g_r(3\gamma-1)}\left[-c_r\left(\frac{\partial g}{\partial\xi}\right)_r + \frac{\gamma+1}{2}\left(\frac{\partial p}{\partial\xi}\right)_r\right]\cdot(\beta^{(3\gamma-1)/2(\gamma+1)}-1). \qquad (B.12_\gamma)$$

APPENDIX C: Additional Details of the Lagrangian Scheme

We provide here the coefficients in Eqs. (5.2), (5.3) for the case that the waves are not as shown in Fig. 3.

(i) The wave travelling to the left is a shock. Instead of Eq. (5.4) we now have, using a γ-law relation,

$$a_l = 2 + A(p^* - p_l), \tag{C.1$_\gamma$}$$

$$b_l = -[A(u^* - u_l) + (g_l^*)^{-2} W_l + W_l^{-1}], \tag{C.2$_\gamma$}$$

$$d_l = L_u \left(\frac{\partial u}{\partial \xi}\right)_l - L_p \left(\frac{\partial p}{\partial \xi}\right)_l - L_\rho \left(\frac{\partial \rho}{\partial \xi}\right)_l, \tag{C.3$_\gamma$}$$

where $W_l = (p^* - p_l)/(u^* - u_l)$,

$$A = -\tfrac{1}{2}(p^* + \mu^2 p_l)^{-1}, \qquad B = (p^* - p_l)^{-1} - \mu^2 A,$$

$$L_u = \rho_l (u^* - u_l)(\gamma p_l B + \tfrac{1}{2}) + W_l, \tag{C.4$_\gamma$}$$

$$L_p = 1 + B(p^* - p_l), \qquad L_\rho = (2\rho_l)^{-1}(p^* - p_l).$$

(ii) The wave travelling to the right is a rarefaction. Instead of Eqs. (5.5$_\gamma$)–(5.8$_\gamma$), we now have

$$a_r = -1, \qquad b_r = (g_r^*)^{-1}, \qquad d_r = -(g_r g_r^*)^{1/2} a(\beta^*), \tag{C.5}$$

where $\beta^* = g_r^*/g_r$ and $a(\beta)$ is now given by (B.12$_\gamma$) (for a γ-law relation).

With the coefficients of (5.2), (5.3) given in all cases, the Lagrangian scheme proceeds as described in Section 6.

APPENDIX D: Additional Details of the Eulerian Scheme

The nonsonic case was fully described in Section 7. We give here the analogues of Eqs. (7.8), (7.9) for the case that the waves are not as shown in Fig. 3.

(i) The wave travelling to the left is a shock. Instead of Eq. (7.8) we obtain

$$\left(\frac{\partial \rho}{\partial \xi}\right)_l^* = 3(\rho_l^*)^2 W_l^{-2} \left(\frac{\partial u}{\partial t}\right)^* - (3(c_l^*)^{-2} W_l^{-1} + (\rho_l^*)^2 W_l^{-3}) \left(\frac{\partial p}{\partial t}\right)^*$$

$$- (3 + g_l^2 W_l^{-2})(\rho_l^*)^2 W_l^{-1} \left(\frac{\partial u}{\partial \xi}\right)_l$$

$$+ 3(\rho_l^*)^2 W_l^{-2} \left(\frac{\partial p}{\partial \xi}\right)_l + (\rho_l^*/\rho_l)^2 \left(\frac{\partial \rho}{\partial \xi}\right)_l. \tag{D.1}$$

(ii) The wave travelling to the right is a rarefaction. Instead of Eq. (7.9) we have

$$\left(\frac{\partial \rho}{\partial \xi}\right)_r^* = (\beta^*)^{-1/2} \frac{\partial \rho(0, \beta^*)}{\partial \alpha} - (g_r^*)^{-1}(c_r^*)^{-2} \left(\frac{\partial p}{\partial t}\right)^*. \tag{D.2}$$

In (D.1), (D.2) we take $W_l = (p^* - p_l)/(u^* - u_l)$, $\beta^* = g_r^*/g_r$, and $\partial\rho(0, \beta)/\partial\alpha$ is obtained in (D.2) from (4.21) or (4.22_γ) by reflecting $(\alpha, \xi, u) \to (-\alpha, -\xi, -u)$, $(p, \rho, g, \beta) \to (p, \rho, g, \beta)$, changing l to r and, for the γ-law, using $(B.12_\gamma)$.

ACKNOWLEDGMENTS

Our starting point in this work was definitely van Leer's important work [11]. He has also kindly made his handwritten notes available to us, which helped us understand the connection between our works and establish the results of Appendix A. It is also a pleasure to thank P. Colella and A. Harten for many useful discussions concerning various aspects of this work.

REFERENCES

1. A. J. CHORIN, Random choice solutions of hyperbolic systems, *J. Comput. Phys.* **22** (1976), 517–533.
2. P. COLELLA, "A Direct Eulerian MUSCL Scheme for Gas Dynamics," Lawrence Berkeley Laboratory LBL-14104, 1982.
3. P. COLELLA AND P. L. WOODWARD, "The Piecewise-Parabolic Method (PPM) for Gas-Dynamical Simulations," Lawrence Berkeley Laboratory LBL-14661, 1982.
4. P. COLELLA AND P. R. WOODWARD, "The Numerical Simulation of Two-Dimensional Fluid Flows with Strong Shocks," Lawrence Livermore National Laboratory Report UCRL-86952, 1982.
5. R. COURANT AND K. O. FRIEDRICHS, "Supersonic Flow and Shock Waves," Interscience, New York, 1948.
6. R. COURANT AND D. HILBERT, "Methods of Mathematical Physics, II," Interscience, New York, 1962.
7. S. K. GODUNOV, A finite difference method for the numerical computation and discontinuous solutions of the equations of fluid dynamics, *Mat. Sb.* **47** (1959), 271–295.
8. A. HARTEN, High resolution schemes for hyperbolic conservation laws, *J. Comput. Phys.* **49** (1983), 357–393.
9. A. HARTEN, On second order accurate Godunov-type schemes, preprint.
10. G. A. SOD, A survey of several finite difference methods for systems of non-linear hyperbolic conservation laws, *J. Comput. Phys.* **27** (1978), 1–31.
11. B. VAN LEER, Towards the ultimate conservative difference scheme, V, *J. Comput. Phys.* **32** (1979), 101–136.